Analysis of Active Lava Flows on Kilauea Volcano, Hawaii, Using SIR-C Radar Correlation Measurements

Howard A. Zebker, Paul Rosen, Scott Hensley

Jet Propulsion Laboratory
California Institute of Technology
Pasadena, CA 91109

and

Peter J. Mouginis-Mark

Hawaii Institute of Geophysics and Planetology
University of Hawaii, Manoa
Honolulu, Hawaii 96822

Submitted to:

Science

August 7, 1995

Please address editorial correspondence to:

Howard A. Zebker
300-227
Jet Propulsion Laboratory
4800 Oak Grove Drive
Pasadena, CA 91109
Tel: (81 8)354-8780
Fax: (81 8)393-5285
Email: zebker@jakey.jpl.nasa.gov

Abstract

Precise eruption rates of active pahoehoe lava flows on Kilauea volcano, Hawaii, have been determined using spaceborne radar data acquired by the Space Shuttle Imaging Radar-C (SIR-C) . A coastal site downslope from the Pu'u O'o vent was imaged once per day, on each of the four days from October 7-10, 1995. Day-to-day decorrelation due to resurfacing was determined by interferometric combination of the data at 15 m resolution over a wide area. On successive days, 335,700 m^2, 368,775 m^2, and 356,625 m^2 of new lava was erupted Assuming an average pahoehoe flow thickness of 50 cm, a mean effusion rate for this period is 1.94 to 2.13 m^3/sec. The radar observations show persistant surface activity at each site, rather than downslope migration of the lava.

Introduction

Measurement of the rate of lava flow advance, and the determination of the volume of new material erupted in a given period of time, are among the most important observations that can be made when studying on-going activity at a volcano (1). In the field, obtaining these parameters is often quite challenging even on the safest of volcanoes, due to the large area over which a flow might advance, the rugged nature of the pre-existing terrain, and the similarity in morphology between newly formed lava and pre-existing surfaces. Monitoring the advance of pahoehoe flows that are spreading sluggishly over nearly flat ground can be particularly challenging as new outbreaks of lava may take place on time scales of a few tens of minutes over a flow field several square kilometers in size.

The formation of new pahoehoe is not only limited to the leading edge of the flow. Break-outs can occur from tumuli located within the central region of the flow (2) and new material can be intruded into a flow during post-emplacement inflation (3). Given the very high temperatures that prevent direct measurement of intra-flow activity, heat shimmer that precludes confident visual identification of all new lava, and the reactivation and inflation of existing flows, a method for the determination of surface change on active lava flows has been lacking until now.

Here we describe a technique utilizing orbital Space Shuttle Imaging Radar (SIR-C) data to map changes in the lava flow field during early October 1994. Since active flows disturb the ground surface by burial of older landscapes, the radar echoes from these areas are essentially uncorrelated between radar observations. However, the surrounding areas correlate quite well, particularly at the longest of the three available radar wavelengths (24, 6, and 3 cm). Thus, the active flow regions may be discerned by plotting the correlation coefficient of the surface at each resolved point. Daily progress of the flow, as well as intra-flow activity, may be monitored by constructing a time series of observations. The area and change in area of the flow field is measured quantitatively by the radar correlation , so by employing typical flow thicknesses as observed in the field to constrain flow volume, these flow measurements provide insights to the mass eruption rate of Kilauea over time scales and areas that hitherto have not been possible.

Correlation measurements

Radar images depict the amount of energy reflected back to the sensor from each resolution element on a surface. For a spaceborne imaging radar, the resolution element ("pixel") is typically a few tens of meters in size, and a swath tens of kilometers wide up to hundreds of kilometers long is acquired. Details of the surface geophysical properties are expressed in the amplitude and phase of the complex backscattered radar echo.

A radar scatterer has a size typically several wavelengths in size, and since most radars operate in the 1 to 100 cm wavelength region of the spectrum, a 15 m by 15 m pixel from a natural surface contains many individual and generally independent scatterers. The radar signal from the pixel is comprised of the coherent sum of the echoes from each of the individual scattering elements therein. If the collection of scatterers is imaged a second time from an identical viewpoint, as is the case for the October 1994 SIR-C repeat orbit experiment, this coherent sum will remain unchanged (4,5). If, however, the scatterers are moved or, as in the case of active lava flows, replaced with a new set of scatterers, the echoes from the resolution element will be uncorrelated with those acquired before the

surface was modified, with the degree of correlation related to the amount of change in the scatterers (6).

Unlike for radar reflectivity measurements, new flows are easily identified in radar correlation maps. In the case of an on-going eruption, the radar reflectivity properties of recent lavas may remain quite similar for long periods of time, typically a few years. Since the radar reflectivity is determined mainly by the statistics of the surface height and slope distribution, a radar image of a new flow is often virtually indistinguishable from an image of a morphologically similar flow that was emplaced a few hours to many months earlier. However, because the correlation of the radar signals from observation to observation depends on the actual realization of the height and slope distribution of the flow surface, rather than its collective statistical description, new flows are easily identified in the correlation maps, (7)

Since decorrelation in the radar returns must be associated with a total change in the distribution of surface scatterers, the individual flows are not simply inflated from beneath, as has been observed for other Kilauea flow fields (3); inflation alone does not result in decorrelation.

The observed signal correlation depends strongly on all motions within a pixel, not just moving lava flows. Other sources of motion could be, for example, vegetation or land cover that changes on the wavelength size scale with time, or the effects of surface moisture that change the details of the radar scattering centers. We have attempted to minimize these additional motion effects by studying radar data with shortest available temporal interval between observations. Since the radar echoes are sensitive mostly to scatterers that are wavelength size and greater, choosing the largest wavelength helps minimize the contaminating motion signals yet preserves sensitivity to the complete redistribution of the surface that results from new flow activity. While regions consisting of bare lava flows correlate strongly, vegetated areas in particular exhibit some motion and hence the correlation decreases. Identifying the decorrelated regions that are indeed active flows can

be aided by field observations, or with time series analysis to discern growing or shrinking areas of correlation that are likely to be the result of active lava flows.

Observations

Correlation data for this study were acquired on October 7- 10, 1994, during the second SIR-C mission, aboard the space shuttle Endeavor in a 205 km altitude one-day exact repeat orbit.

The one-day repeat interval observations are shown in Figure 1, depicting a 100 km by 21 km swath extending from near the summit of Mauna Kea, then across the upper East Rift Zone of Kilauea region near the Pu'u O'o cone, to the Pacific Ocean. Data are presented for time intervals of October 7-8, 8-9, and 9-10, resulting in three successive one day correlation intervals. The track angle of the swath is oriented 146.5° with respect to north. Expansion of the active flow areas is shown in Figure 2, each corresponding to about 3.8 km by 3.8 km on the ground. These data were resampled to UTM coordinates using a USGS 30 m posting digital elevation model (DEM) for topographic correction (8). The active lava flows are seen as decorrelated features in the lower part of the images, Other areas of significant decorrelation are also visible, and these are related to small-scale movements in the vegetation cover and to the presence of ocean surface in the lower left corner.

Table 1 contains area measurements of the flows obtained by counting the number of 15 m x 15 m pixels contained in each decorrelated region (9). The decorrelated features are grouped into three principal flows, as denoted by Regions 1 to 3 in Figure 2. Table 1 gives the total areal measurements for each flow, obtained by adding the contributions for each small subregion (1 O). Also given are estimates of the daily lava volume from each flow, obtained by assuming a flow thickness of 0.5 m. This value is reasonable given our field observations of the growing pahoehoe flow field that we made on October 9th concurrent with the radar observations. Although this is only an approximation, pahoehoe flows rarely exceed 1 m thickness prior to inflation, and are never less than -20 cm thick (3). Finally, the inferred total daily effusion rates are listed,

Interpretation

The key attributes of the entire flow field that we can derive from these radar correlation studies are two-fold. First, Figure 2 shows that the locations of surface activity remained almost constant throughout the observation period. Although for Flow Region #1 the area of current activity diminished in size between the start and end of the observations, it remained active all the time, while the area of activity associated with Flow Regions #2 and #3 actually grew in size (1 1).

Secondly, referring again to Figure 2, we divide the areas of decorrelation (that is, surface activity) into three regions in Table 1 for convenience. We recognize that these surface break-outs originate from three segments of the same active flow field. From the volumes of new material we derive an estimate of the mass eruption rate for this part of the volcano, assuming that the density of the material is also known. Table 1 shows that 335,700 m^2, 368,775 m^2, and 356,625 m^2 of new lava was erupted on the successive days. Taking 50 cm as the average thickness of new pahoehoe flows, these values translate to 167,850 m^3, 184,388 m^3 and 178,313 m^3 per day, equivalent to eruption rates of 1.94 m^3/sec, 2.13 m^3/sec and 2.06 m^3/sec for the three days. Such values are close to the ~3 -4 m^3/sec cited by U.S. Geological Survey scientists making near-vent observations on the eruptions at Kilauea (12, 13). Lower values are also consistent with field observations on October 8th and 9th that new lava was also entering the ocean via lava tubes during the four day period in question, as evidenced by large steam plumes. The three independent effusion rate estimates for the three 24-hour periods are also remarkably similar, indicating that activity at Kilauea remained consistent for the period of our observations.

Conclusions

From the estimated area and mass rates and the spatial distribution of the decorrelated areas, we can identify persistent activity from the same pseudo-vents on the

Kilauea flow field, rather than the migration of individual flows downslope. These results demonstrate that interferometric radar analyses of new lava fields provide a level of precision exceeding that of conventional field studies. Furthermore, in inaccessible regions the technique may be expected to perform equally well, While the radar provides high precision areal measurements, the availability of field observations such as flow thickness and viscosity increase geologic understanding. Our results also raise the possibility of the identification of the areas of change associated with pyroclastic volcanism, such as the formation or growth of cinder cones, the collapse of summit craters, changes in the morphology of lahar deposits due to erosion and/or deposition, and the measurement of the area of pyroclastic materials formed by more explosive eruptions. In this last example, radar interferometry may eventually provide a remote sensing method for producing isopach maps (15) for the ash produced by new eruptions. We therefore conclude that, since field work in areas of active volcanism can be expensive, time-consuming, logistically challenging and dangerous for those involved, the radar interferometry method presented here offers the potential of great insight into the magnitude and distribution of volcanic processes associated with new eruptions.

References

1. Tilling, R. 1. and D. W. Peterson (1 993). Field observation of active lava in Hawaii: some practical considerations. In: Active *Lavas*, C. R. J. Kilburn and G. Luongo, Eds., UCL Press, London, pp. 147- 174.

2. Walker, G. P. L. (1991), Bulletin Volcanology, 53, 546-558.

3. t-fen, K.$_s$ J. Kauahikaua, R. Denlinger, and K. MacKay (1994), Hawaii. Geol. Sot. Amer. Bull., 106, 351 -370.

4. Li, F. and R. M. Goldstein, IEEE Trans. Geosci. Rem. Sens., Vol. 28, no. 1, pp. 88-97, January 1990.

5. Zebker, H. A., and J. Villasenor, IEEE Trans. Geosci. Rem. Sensi., Vol 30, no. 5, pp. 950-959, September, 1992.

6. The coherent sum signal depends also on the exact imaging geometry, hence other sensor-related effects alter the correlation properties of the signals. These other factors, which include the difference in radar look angle (or interferometric baseline), signal to noise ratio, and influence of vegetation or other variable surface cover, must be considered in analysis of the correlation data, For a more complete discussion of these and other radar correlation properties, see (5) or (Rodriguez, E., J.M. Martin, IEE Proceedings-F, Vol. 139, No. 2, pp. 147-159, April 1992.) Interested readers may see (Gatelli, F., A. Monti Guarnieri, F. Parizzi, P. Pasquali, C. Prati, F. Rocca, IEEE Trans. Geosci. Rem. Sensi., Vol 32, no 4, pp. 855-865, July 1994) for demonstration of methods to reduce or eliminate the non-motion contributors to correlation.

7. The correlation measurements reported here are derived using the following equation:

$$c = \frac{E(s_1 s_2^*)}{\sqrt{E(s_1 s_1^*)E(s_2 s_2^*)}}$$

where the correlation is denoted by c, s_1 and S_2 are the complex signal values from the two radar images, and the expectation E( ) is evaluated by a spatial average.

Since the correlation values as defined above are both statistical and biased, some care must be exercised in interpreting the results in terms of surface change. For example, in Figure footnote-7 we plot theoretical probability distribution functions for the correlation coefficient when the underlying signals s, and s_2 are completely uncorrelated and also when they are correlated at the 900/' level. Each of these instances is plotted twice, assuming 10 and 40 independent observations ("looks") . Since we obtain looks via spatial averaging, a processing tradeoff exists between spatial resolution and accuracy of the correlation measurement.

8. The USGS DEM was acquired before the current series of activity began in 1983, so for accuracy we inserted a DEM swath derived by the NASA TOPSAR instrument to better account for the altered topography along the East Rift Zone and the area downslope from the Pu'u O'o and Kupaianaha vents (Zebker, H. A., S.N. Madsen, J. Martin, K.B. Wheeler, T. Miller, Y. Lou, G. Alberti, S. Vetrella, A. Cucci, IEEE Trans. Geosci. and Rem. Sens., Vol 30, no. 5, pp 933-940, September, 1992; Madsen, S. N., J. Martin, H.A. Zebker, IEEE Trans. Geosci. and Rem. Sens., Vol. 33, No. 2, pp. 383-391, March 1995.)

9. The decorrelated flow boundaries are determined by a thresholding operation on the observed correlation. We measured the statistics of both the correlated and uncorrelated areas in the images, and chose a threshold that would result in equal probabilities of assigning a pixel from the correlated population uncorrelated status, and also the reverse. The resulting binary maps were used to identify the lava flows, and the number of pixels within each flow were counted. We also measured the perimeter of each flow for use in error analysis.

10. Errors inherent in the radar measurements arise from both systematic and statistical effects. The edge of a decorrelated region is known only to the nearest pixel. We assume that each region is surrounded by an annulus with a width uniformly distributed between zero and one. Thus the systematic uncertainty in the area of this

annulus is the perimeter of the region, multiplied by $\frac{1}{\sqrt{12}}$, times the area of one pixel.

The statistical uncertainty may be approximated by assuming that the edge pixels form draws from a binomial distribution. The standard deviation of the resultant distribution is equal to the square root of perimeter of the region, divided by two, and multiplied by pixel area. The factor of two follows from the parameter of the binomial distribution as determined from our detection algorithm. For each of the three days where change was detected, the resultant systematic error is ranges from 7-160/., while the statistical component of error varies from 0.9 - 3.2%. Additional errors in the volume calculation would follow from an incorrect assumption of the flow thickness.

11. Simple displacement of the surface flow without the emplacement of new material from the subsurface could result in a similar decorrelation signature to that observed in Figure 2. For example, a recently erupted lava flow might continue to move downslope even though the vent that erupted the lava were no longer active. Such motion need only occur for a few minutes after the first radar observation, since it is the total motion over the following 24 hour period that the radar detects. Our field observations show that individual lava flow lobes may stay active for a few tens of minutes, but that the individual flow lobes that were forming on Kilauea on the days in question did not travel more than 15 meters (i.e., 1 radar pixel) after the vent became inactive. Thus our field knowledge of the activity at Kilauea in early October 1994, and our interpretation of the SIR-C measurements, lead us to conclude that over the four days in question, new material was erupted daily from the same sites, and that the location of these active flow lobes did not migrate downslope with the advance of a single flow. If this were the case, such an advance would have been identified by the change in location of the decorrelated areas on a day-by-day basis.

12. Wolfe, E. W., M. O. Garcia, D. B. Jackson, J. Koyanagi, C. A. Neal, A. T. Okamura, The Pu'u 'O'O eruption of Kilauea volcano, episodes 1 - 20, January 3, 1983 to June 8, 1984. In Decker, R. W., T. L. Wright, and P. H. Stauffer (eds). *Volcanism in Hawaii.* US Geological Survey Prof. Paper., 1350, pp. 471 -508, 1987.

13. Mangan, M. T., C. C. Heliker, T. N. Mattox, J. P. Kauahikaua, and R. T. Helz, Bull. Volcanol. 57, 127- 135, 1995,

14. Walker, G. P. L., Geol. Rundsch. 62, 431 -446, 1993.

Table 1. Kilauea **Active Flow Observations Summary**

Time interval	Ott .7-8	Ott .8:9	Oct. 9-1o
Areas, square meters:			
Flow region 1	183375	126225	69975
Flow region 2	122400	154125	175950
Flow region 3	29925	88425	110700
Total daily activity	335700	368775	356625
Volumes, cubic meters:			
Flow region 1	91688	63113	34988
Flow region 2	61200	77063	87975
Flow region 3	14963	44213	55350
Total daily activity	167850	184388	178313
Total effusion rate, cubic meters per second:			
	1.94	2.13	2.06

Figure captions

Figure 1. SIR-C radar data swaths depicting correlation observations for the time intervals of Oct. 7-8, 8-9, and 9-10. Swath size is 100 km by 21 km and ranges from near the peak of Mauna Loa (top), across the upper East Rift Zone of Kilauea, to the Pacific Ocean. A portion of the Chain of Craters area is visible towards the lower part of the image. Correlation coefficient values (color) overlaid on radar brightness values permit feature identification. The data are processed to a multi-look pixel size of 15 m by 15 m in ground coordinates.

Figure 2. Expansion of the active flow area from each of the swaths shown in Figure 1. The flows are easily identified and grouped into three regions. Additional decorrelated areas due to vegetation and water surfaces are also evident. The area shown is 3.8 km by 3.8 km. Flow 1 shows decreased activity with time, while flows 2 and 3 increase. The total resurfaced area remains quite constant over the four day observation period.

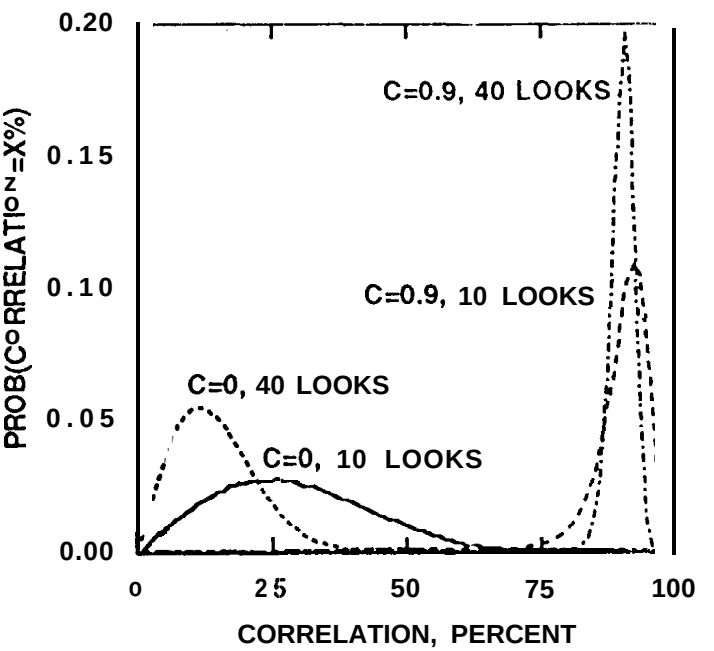

Figure footnote-7. Probability density functions of correlation coefficient for signals that are i) completely uncorrelated and ii) correlated at the 90% level, for both 10 and 40 radar "looks".

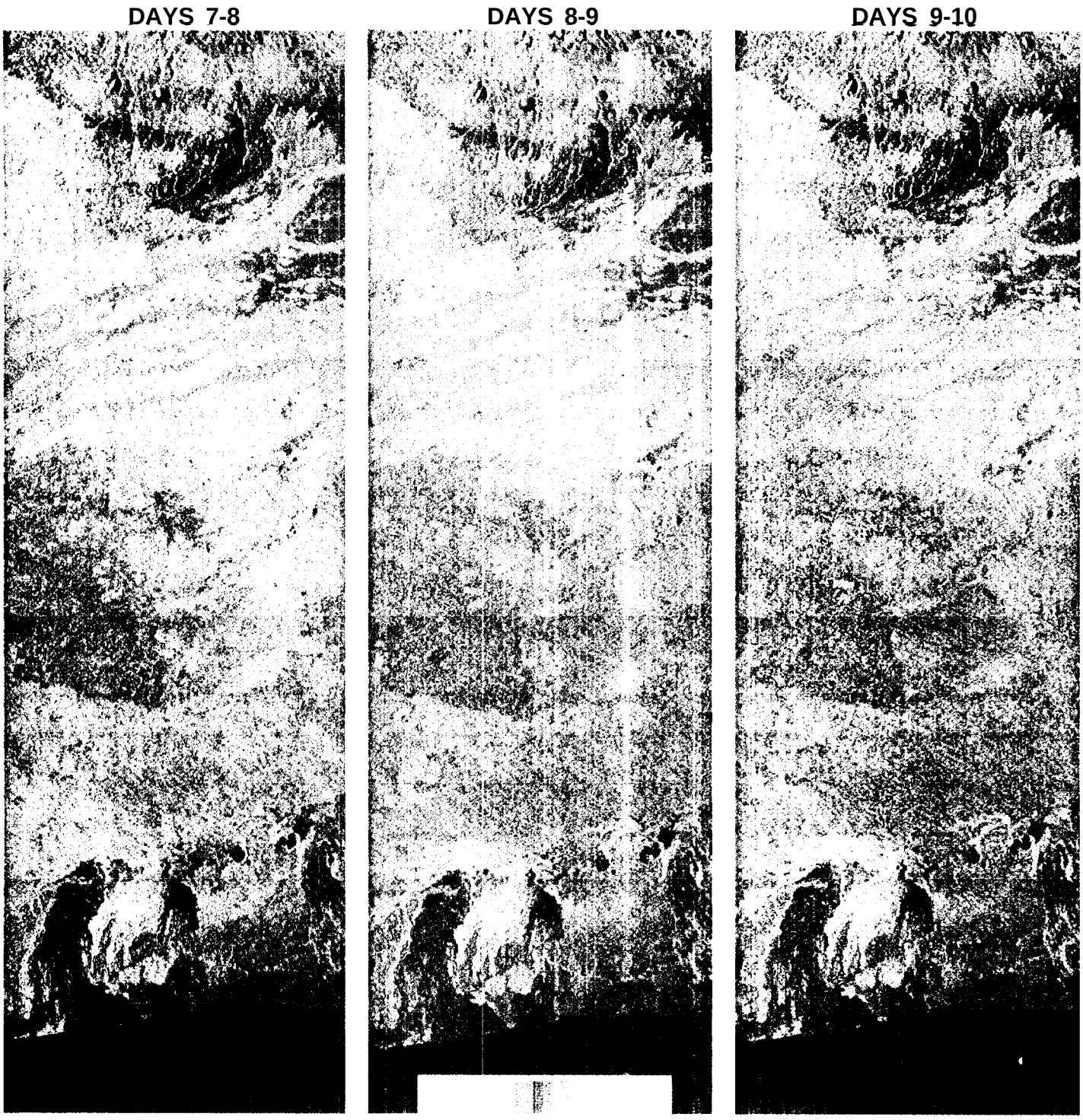

Fig. 1
Zebker et al
1995

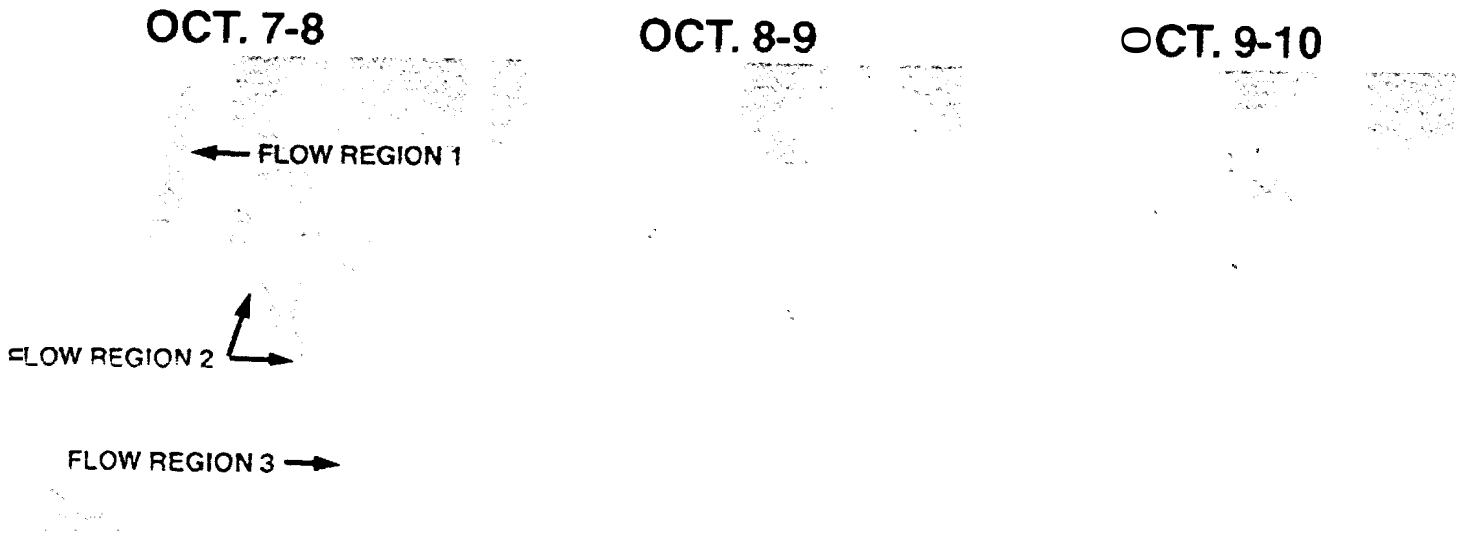

Fig. 2
Zebker et a
1995

Analysis of Active Lava Flows on Kilauea Volcano, Hawaii, Using SIR-C Radar Correlation Measurements

Howard A. Zebker, Paul Rosen, Scott Hensley

Jet Propulsion Laboratory
California Institute of Technology
Pasadena, CA 91109

and

Peter J. Mouginis-Mark

Hawaii Institute of Geophysics and Planetology
University of Hawaii, Manoa
Honolulu, Hawaii 96822

Submitted to:

Science

August 7, 1995

Please address editorial correspondence to:

Howard A. Zebker
300-227
Jet Propulsion Laboratory
4800 Oak Grove Drive
Pasadena, CA 91109
Tel: (81 8)354-8780
Fax: (81 8)393-5285
Email: zebker@jakey.jpl.nasa.gov

Abstract

Precise eruption rates of active pahoehoe lava flows on Kilauea volcano, Hawaii, have been determined using spaceborne radar data acquired by the Space Shuttle Imaging Radar-C (SIR-C) . A coastal site downslope from the Pu'u 0'0 vent was imaged once per day, on each of the four days from October 7-1o, 1995. Day-to-day decorrelation due to resurfacing was determined by interferometric combination of the data at 15 m resolution over a wide area. On successive days, 335,700 m^2, 368,775 m^2, and 356,625 m^2 of new lava was erupted Assuming an average pahoehoe flow thickness of 50 cm, a mean effusion rate for this period is 1.94 to 2.13 m^3/sec. The radar observations show persistant surface activity at each site, rather than downslope migration of the lava.

Introduction

Measurement of the rate of lava flow advance, and the determination of the volume of new material erupted in a given period of time, are among the most important observations that can be made when studying on-going activity at a volcano (l). In the field, obtaining these parameters is often quite challenging even on the safest of volcanoes, due to the large area over which a flow might advance, the rugged nature of the pre-existing terrain, and the similarity in morphology between newly formed lava and pre-existing surfaces. Monitoring the advance of pahoehoe flows that are spreading sluggishly over nearly flat ground can be particularly challenging as new outbreaks of lava may take place on time scales of a few tens of minutes over a flow field several square kilometers in size.

The formation of new pahoehoe is not only limited to the leading edge of the flow. Break-outs can occur from tumuli located within the central region of the flow (2) and new material can be intruded into a flow during post-emplacement inflation (3). Given the very high temperatures that prevent direct measurement of intra-flow activity, heat shimmer that precludes confident visual identification of all new lava, and the reactivation and inflation of existing flows, a method for the determination of surface change on active lava flows has been lacking until now.

Here we describe a technique utilizing orbital Space Shuttle Imaging Radar (SIR-C) data to map changes in the lava flow field during early October 1994. Since active flows disturb the ground surface by burial of older landscapes, the radar echoes from these areas are essentially uncorrelated between radar observations. However, the surrounding areas correlate quite well, particularly at the longest of the three available radar wavelengths (24, 6, and 3 cm). Thus, the active flow regions may be discerned by plotting the correlation coefficient of the surface at each resolved point. Daily progress of the flow, as well as intra-flow activity, may be monitored by constructing a time series of observations. The area and change in area of the flow field is measured quantitatively by the radar correlation , so by employing typical flow thicknesses as observed in the field to constrain flow volume, these flow measurements provide insights to the mass eruption rate of Kilauea over time scales and areas that hitherto have not been possible.

Correlation measurements

Radar images depict the amount of energy reflected back to the sensor from each resolution element on a surface. For a spaceborne imaging radar, the resolution element ("pixel") is typically a few tens of meters in size, and a swath tens of kilometers wide up to hundreds of kilometers long is acquired. Details of the surface geophysical properties are expressed in the amplitude and phase of the complex backscattered radar echo.

A radar scatterer has a size typically several wavelengths in size, and since most radars operate in the 1 to 100 cm wavelength region of the spectrum, a 15 m by 15 m pixel from a natural surface contains many individual and generally independent scatterers. The radar signal from the pixel is comprised of the coherent sum of the echoes from each of the individual scattering elements therein. If the collection of scatterers is imaged a second time from an identical viewpoint, as is the case for the October 1994 SIR-C repeat orbit experiment, this coherent sum will remain unchanged (4,5). If, however, the scatterers are moved or, as in the case of active lava flows, replaced with a new set of scatterers, the echoes from the resolution element will be uncorrelated with those acquired before the

surface was modified, with the degree of correlation related to the amount of change in the scatterers (6).

Unlike for radar reflectivity measurements, new flows are easily identified in radar correlation maps. In the case of an on-going eruption, the radar reflectivity properties of recent lavas may remain quite similar for long periods of time, typically a few years. Since the radar reflectivity is determined mainly by the statistics of the surface height and slope distribution, a radar image of a new flow is often virtually indistinguishable from an image of a morphologically similar flow that was emplaced a few hours to many months earlier. However, because the correlation of the radar signals from observation to observation depends on the actual realization of the height and slope distribution of the flow surface, rather than its collective statistical description, new flows are easily identified in the correlation maps. (7)

Since decorrelation in the radar returns must be associated with a total change in the distribution of surface scatterers, the individual flows are not simply inflated from beneath, as has been observed for other Kilauea flow fields (3); inflation alone does not result in decorrelation.

The observed signal correlation depends strongly on all motions within a pixel, not just moving lava flows. Other sources of motion could be, for example, vegetation or land cover that changes on the wavelength size scale with time, or the effects of surface moisture that change the details of the radar scattering centers, We have attempted to minimize these additional motion effects by studying radar data with shortest available temporal interval between observations. Since the radar echoes are sensitive mostly to scatterers that are wavelength size and greater, choosing the largest wavelength helps minimize the contaminating motion signals yet preserves sensitivity to the complete redistribution of the surface that results from new flow activity. While regions consisting of bare lava flows correlate strongly, vegetated areas in particular exhibit some motion and hence the correlation decreases. Identifiying the decorrelated regions that are indeed active flows can

be aided by field observations, or with time series analysis to discern growing or shrinking areas of correlation that are likely to be the result of active lava flows.

Observations

Correlation data for this study were acquired on October 7- 10, 1994, during the second SIR-C mission, aboard the space shuttle Endeavor in a 205 km altitude one-day exact repeat orbit.

The one-day repeat interval observations are shown in Figure 1, depicting a 100 km by 21 km swath extending from near the summit of Mauna Kea, then across the upper East Rift Zone of Kilauea region near the Pu'u O'o cone, to the Pacific Ocean. Data are presented for time intervals of October 7-8, 8-9, and 9-10, resulting in three successive one day correlation intervals. The track angle of the swath is oriented 146.5° with respect to north. Expansion of the active flow areas is shown in Figure 2, each corresponding to about 3.8 km by 3.8 km on the ground. These data were resampled to UTM coordinates using a USGS 30 m posting digital elevation model (DEM) for topographic correction (8). The active lava flows are seen as decorrelated features in the lower part of the images. Other areas of significant decorrelation are also visible, and these are related to small-scale movements in the vegetation cover and to the presence of ocean surface in the lower left corner.

Table 1 contains area measurements of the flows obtained by counting the number of 15 m x 15 m pixels contained in each decorrelated region (9). The decorrelated features are grouped into three principal flows, as denoted by Regions 1 to 3 in Figure 2. Table 1 gives the total areal measurements for each flow, obtained by adding the contributions for each small subregion (1 O). Also given are estimates of the daily iava volume from each flow, obtained by assuming a flow thickness of 0.5 m. This value is reasonable given our field observations of the growing pahoehoe flow field that we made on October 9th concurrent with the radar observations. Although this is only an approximation, pahoehoe flows rarely exceed 1 m thickness prior to inflation, and are never iess than -20 cm thick (3). Finally, the inferred total daily effusion rates are listed.

Interpretation

The key attributes of the entire flow field that we can derive from these radar correlation studies are two-fold. First, Figure 2 shows that the locations of surface activity remained almost constant throughout the observation period. Although for Flow Region #1 the area of current activity diminished in size between the start and end of the observations, it remained active all the time, while the area of activity associated with Flow Regions #2 and #3 actually grew in size (11).

Secondly, referring again to Figure 2, we divide the areas of decorrelation (that is, surface activity) into three regions in Table 1 for convenience. We recognize that these surface break-outs originate from three segments of the same active flow field. From the volumes of new material we derive an estimate of the mass eruption rate for this part of the volcano, assuming that the density of the material is also known. Table 1 shows that 335,700 m^2, 368,775 m^2, and 356,625 m^2 of new lava was erupted on the successive days. Taking 50 cm as the average thickness of new pahoehoe flows, these values translate to 167,850 m^3, 184,388 m^3 and 178,313 m^3 per day, equivalent to eruption rates of 1.94 m^3/sec, 2.13 m^3/sec and 2.06 m^3/sec for the three days. Such values are close to the ~3 - 4 m^3/sec cited by U.S. Geological Survey scientists making near-vent observations on the eruptions at Kilauea (12, 13). Lower values are also consistent with field observations on October 8th and 9th that new lava was also entering the ocean via lava tubes during the four day period in question, as evidenced by large steam plumes. The three independent effusion rate estimates for the three 24-hour periods are also remarkably similar, indicating that activity at Kilauea remained consistent for the period of our observations.

Conclusions

From the estimated area and mass rates and the spatial distribution of the decorrelated areas, we can identify persistent activity from the same pseudo-vents on the

Kilauea flow field, rather than the migration of individual flows downslope. These results demonstrate that interferometric radar analyses of new lava fields provide a level of precision exceeding that of conventional field studies. Furthermore, in inaccessible regions the technique may be expected to perform equally well. While the radar provides high precision areal measurements, the availability of field observations such as flow thickness and viscosity increase geologic understanding. Our results also raise the possibility of the identification of the areas of change associated with pyroclastic volcanism, such as the formation or growth of cinder cones, the collapse of summit craters, changes in the morphology of lahar deposits due to erosion and/or deposition, and the measurement of the area of pyroclastic materials formed by more explosive eruptions. In this last example, radar interferometry may eventually provide a remote sensing method for producing isopach maps (15) for the ash produced by new eruptions. We therefore conclude that, since field work in areas of active volcanism can be expensive, time-consuming, logistically challenging and dangerous for those involved, the radar interferometry method presented here offers the potential of great insight into the magnitude and distribution of volcanic processes associated with new eruptions.

References

1. Tilling, R. 1. and D. W. Peterson (1 993). Field observation of active lava in Hawaii: some practical considerations. In: Active *Lavas*, C. R. J. Kilburn and G. Luongo, Eds., UCL Press, London, pp. 147-174.

2. Walker, G. P. L. (1 991), Bulletin Volcanology, 53, 546-558.

3. Hen, K., J. Kauahikaua, R. Denlinger, and K. MacKay (1994), Hawaii. Geol. Sot. Amer. Bull., 106, 351 -370.

4. Li, F. and R. M. Goldstein, IEEE Trans. Geosci. Rem. Sens., Vol. 28, no. 1, pp. 88-97, January 1990.

5. Zebker, H. A., and J. Villasenor, IEEE Trans. Geosci. Rem. Sensi., Vol 30, no. 5, pp. 950-959, September, 1992.

6. The coherent sum signal depends also on the exact imaging geometry, hence other sensor-related effects alter the correlation properties of the signals. These other factors, which include the difference in radar look angle (or interferometric baseline), signal to noise ratio, and influence of vegetation or other variable surface cover, must be considered in analysis of the correlation data. For a more complete discussion of these and other radar correlation properties, see (5) or (Rodriguez, E., J.M. Martin, IEE Proceedings-F, Vol. 139, No. 2, pp. 147-159, April 1992.) Interested readers may see (Gatelli, F., A. Monti Guarnieri, F. Parizzi, P. Pasquali, C. Prati, F. Rocca, IEEE Trans. Geosci. Rem. Sensi., Vol 32, no 4, pp. 855-865, July 1994) for demonstration of methods to reduce or eliminate the non-motion contributors to correlation.

7. The correlation measurements reported here are derived using the following equation:

$$c = \frac{E(s_1 s_2^*)}{\sqrt{E(s_1 s_1^*)E(s_2 s_2^*)}}$$

where the correlation is denoted by c, s, and s_2 are the complex signal values from the two radar images, and the expectation E( ) is evaluated by a spatial average.

Since the correlation values as defined above are both statistical and biased, some care must be exercised in interpreting the results in terms of surface change. For example, in Figure footnote-7 we plot theoretical probability distribution functions for the correlation coefficient when the underlying signals s, and s_2 are completely uncorrelated and also when they are correlated at the 90% level. Each of these instances is plotted twice, assuming 10 and *40* independent observations ("looks") . Since we obtain looks via spatial averaging, a processing tradeoff exists between spatial resolution and accuracy of the correlation measurement.

8. The USGS OEM was acquired before the current series of activity began in 1983, so for accuracy we inserted a OEM swath derived by the NASA TOPSAR instrument to better account for the aftered topography along the East Rift Zone and the area downslope from the Pu'u O'o and Kupaianaha vents (Zebker, H. A., S.N. Madsen, J. Martin, K.B. Wheeler, T. Miller, Y. Lou, G. Alberti, S. Vetrella, A. Cucci, IEEE Trans. Geosci. and Rem. Sens., Vol 30, no. 5, pp *933-940,* September, 1992; Madsen, S. N., J. Mar-tin, H.A. Zebker, IEEE Trans. Geosci. and Rem. Sens., Vol. *33, No. 2,* pp. 383-391, March 1995.)

9. The decorrelated flow boundaries are determined by a thresholding operation on the observed correlation. We measured the statistics of both the correlated and uncorrelated areas in the images, and chose a threshold that would result in equal probabilities of assigning a pixel from the correlated population uncorrelated status, and also the reverse. The resulting binary maps were used to identify the lava flows, and the number of pixels within each flow were counted. We also measured the perimeter of each flow for use in error analysis.

10. Errors inherent in the radar measurements arise from both systematic and statistical effects. The edge of a decorrelated region is known only to the nearest pixel. We assume that each region is surrounded by an annulus with a width uniformly distributed between zero and one. Thus the systematic uncertainty in the area of this

annulus is the perimeter of the region, multiplied by $\frac{1}{\sqrt{12}}$, times the area of one pixel.

The statistical uncertainty may be approximated by assuming that the edge pixels form draws from a binomial distribution. The standard deviation of the resultant distribution is equal to the square root of perimeter of the region, divided by two, and multiplied by pixel area. The factor of two follows from the parameter of the binomial distribution as determined from our detection algorithm. For each of the three days where change was detected, the resultant systematic error is ranges from 7-16%, while the statistical component of error varies from 0.9- 3.2%. Additional errors in the volume calculation would follow from an incorrect assumption of the flow thickness.

11. Simple displacement of the surface flow without the emplacement of new material from the subsurface could result in a similar decorrelation signature to that observed in Figure 2. For example, a recently erupted lava flow might continue to move downslope even though the vent that erupted the lava were no longer active. Such motion need only occur for a few minutes after the first radar observation, since it is the total motion over the following 24 hour period that the radar detects. Our field observations show that individual lava flow lobes may stay active for a few tens of minutes, but that the individual flow lobes that were forming on Kilauea on the days in question did not travel more than 15 meters (i.e., 1 radar pixel) after the vent became inactive. Thus our field knowledge of the activity at Kilauea in early October 1994, and our interpretation of the SIR-C measurements, lead us to conclude that over the four days in question, new material was erupted daily from the same sites, and that the location of these active flow lobes did not migrate downslope with the advance of a single flow. If this were the case, such an advance would have been identified by the change in location of the decorrelated areas on a day-by-day basis.

12. Wolfe, E. W., M. O. Garcia, D. B. Jackson, J. Koyanagi, C. A. Neal, A. T. Okamura, The Pu'u 'O'o eruption of Kilauea volcano, episodes 1 -20, January 3, 1983 to June 8, 1984. In : Decker, R. W., T. L. Wright, and P. H. Stauffer (eds). *Volcanism in Hawaii,* US Geological Survey Prof. Paper., 1350, pp. 471 -508, 1987.

13. Mangan, M. T., C. C. Heliker, T. N. Mattox, J. P. Kauahikaua, and R. T. Helz, Bull. Volcanol. 57, 127-135, 1995.

14. Walker, G. P. L., Geol. Rundsch. 62, 431 -446, 1993.

Table 1. Kilauea **Active Flow Observations Summary**

Time interval	Oct. 7-8	Oct. 8-9	Oct. 9-1o
Areas, square meters:			
Flow region 1	183375	126225	69975
Flow region 2	122400	154125	175950
Flow region 3	29925	88425	110700
Total daily activity	335700	368775	356625
Volumes, cubic meters:			
Flow region 1	91688	63113	34988
Flow region 2	61200	77063	87975
Flow region 3	14963	44213	55350
Total daily activity	167850	184388	178313
Total effusion rate, cubic meters per second:			
	1.94	2.13	2.06

Figure captions

Figure 1. SIR-C radar data swaths depicting correlation observations for the time intervals of Oct. 7-8, 8-9, and 9-10. Swath size is 100 km by 21 km and ranges from near the peak of Mauna Loa (top), across the upper East Rift Zone of Kilauea, **to the Pacific Ocean. A portion of the Chain of Craters area is visible towards the lower part of the image. Correlation coefficient values (color) overlaid on radar brightness values permit feature identification. The data are** processed **to a multi-look pixel size of 15 m by 15 m in ground coordinates.**

Figure 2. Expansion of the active flow area from each of the swaths shown in Figure 1. The flows are easily identified and grouped into three regions. Additional decorrelated areas due to vegetation and water surfaces are also evident. The area shown is 3.8 km by 3.8 km. **Flow 1 shows** decreased activity **with time, while flows 2 and 3 increase. The total resurfaced area remains quite constant over the four day observation period.**

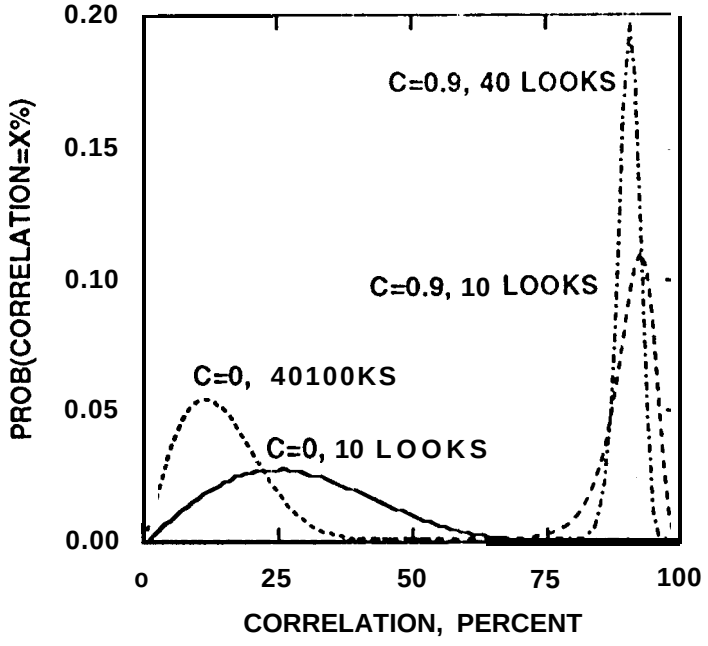

Figure footnote-7. Probability density functions of correlation coefficient for signals that are i) completely uncorrelated and ii) correlated at the 90% level, for both 10 and 40 radar '(looks".

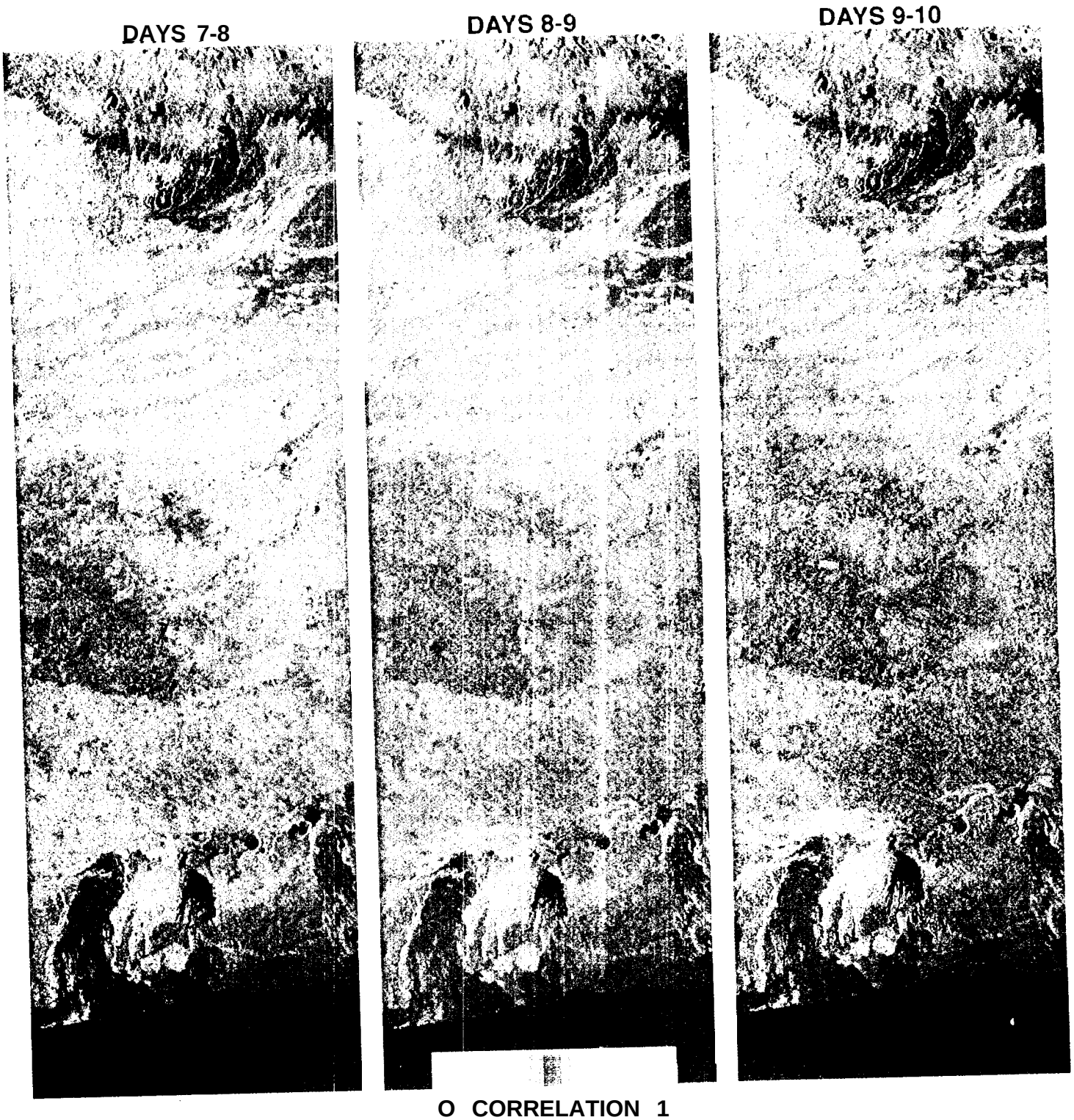

Fig. 1
Zebker **et** al
1995

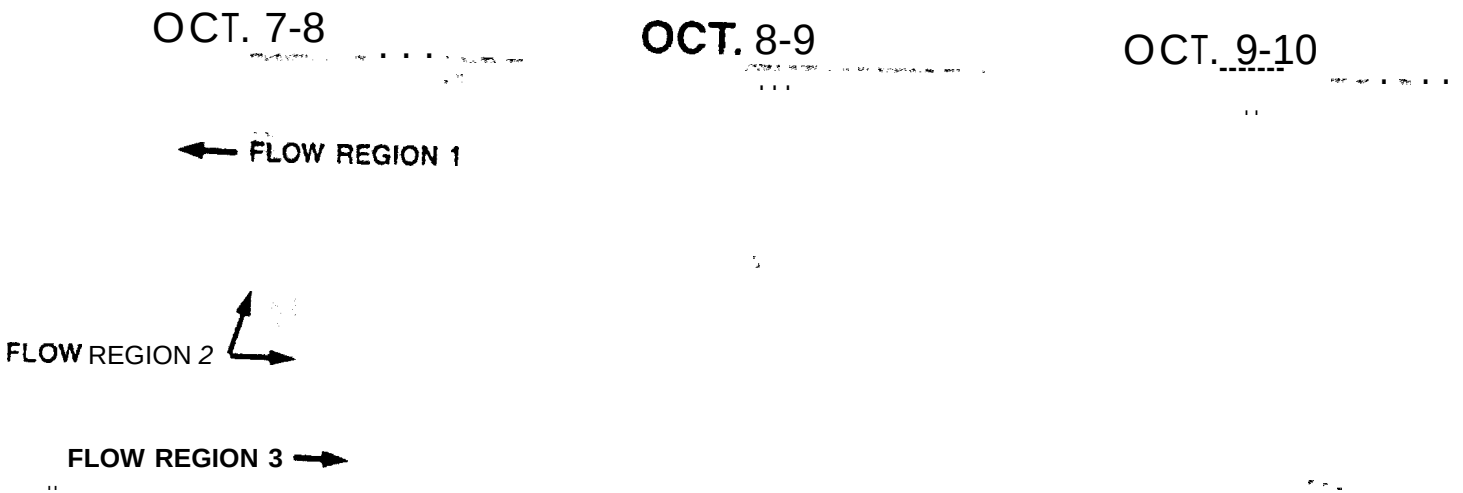

Fig. 2
Zebker et **al**
1995